Continuous Audio Language Models

Simon Rouard[*]
Kyutai
UMR STMS
IRCAM-CNRS Sorbonne Univ.
`simon@kyutai.org`

Manu Orsini[*]
Kyutai
`manu@kyutai.org`

Axel Roebel
UMR STMS
IRCAM-CNRS Sorbonne Univ.

Neil Zeghidour
Kyutai

Alexandre Défossez
Kyutai
`alex@kyutai.org`

Abstract

Audio Language Models (ALM) have emerged as the dominant paradigm for speech and music generation by representing audio as sequences of discrete tokens. Yet, unlike text tokens, which are invertible, audio tokens are extracted from lossy codecs with a limited bitrate. As a consequence, increasing audio quality requires generating more tokens, which imposes a trade-off between fidelity and computational cost. We address this issue by studying Continuous Audio Language Models (CALM). These models instantiate a large Transformer backbone that produces a contextual embedding at every timestep. This sequential information then conditions an MLP that generates the next continuous frame of an audio VAE through consistency modeling. By avoiding lossy compression, CALM achieves higher quality at lower computational cost than their discrete counterpart. Experiments on speech and music demonstrate improved efficiency and fidelity over state-of-the-art discrete audio language models, facilitating lightweight, high-quality audio generation. Samples are available at hf.co/spaces/kyutai/calm-samples.

1 Introduction

Using classification over a finite vocabulary as the training objective for autoregressive sequence models is an effective approach for naturally discrete modalities such as text, where large-scale Transformer-based (Vaswani et al., 2017) language models such as LLaMa (Touvron et al., 2023) and GPT-4 OpenAI (2024) have achieved impressive results. To extend this powerful framework to continuous domains such as image, audio, or video, previous work has mostly relied on discretizing signals using lossy compression algorithms (van den Oord et al., 2018), such that they become akin to text. In particular, neural audio codecs (Zeghidour et al., 2021; Défossez et al., 2024a) have provided discrete representations of audio that are compact enough to allow for high-quality speech (Borsos et al., 2023; Wang et al., 2023) and music (Agostinelli et al., 2023; Copet et al., 2023) generation with autoregressive models. In this context, a Residual Vector Quantizer (RVQ) (Zeghidour et al., 2021) transforms an audio frame into a coarse-to-fine hierarchy of tokens. As quantization inevitably introduces a perceptual quality loss, generating high-fidelity audio requires increasing the bitrate of audio tokens, which amounts to using deeper hierarchies of RVQ tokens. A consequence of growing the size of the token matrix (along time and token depth) is an additional computational load for the generative model, as the strong dependencies between tokens of the same frame(Lemercier et al., 2024) prevent fully parallel generation. The naive approach of flattening the token hierarchy (Borsos et al., 2023)

---

[*]Equal Contribution

being prohibitively expensive, Copet et al. (2023) introduces a delay pattern that conjugates the computational efficiency of parallel generation with a better modeling of inter-token dependencies. Lee et al. (2022) and Yang et al. (2023) furthermore introduce a smaller RQ-Transformer model that is autoregressive along the depth axis, and Défossez et al. (2024b) combines this approach with the delay pattern. While these methods currently power state-of-the-art generative models for audio (Défossez et al., 2024b; Labiausse et al., 2025), the trade-off imposed by residual quantization between quality and computation remains too constraining for generating high-quality audio on edge devices.

This motivates an alternative strategy: autoregressive modeling of continuous latents without quantization. Standard variational autoencoders (VAEs) are easier to train, are not affected by issues such as codebook collapse, and can reconstruct audio at higher fidelity for the same latent dimensionality. Pioneering work in the vision domain that autoregressively models continuous sequences includes GIVT (Tschannen et al., 2024) and MAR (Li et al., 2024), followed by some larger models in the image domain (Fan et al., 2025; Gu et al., 2025) and attempts in the audio domain (Turetzky et al., 2024; Pasini et al., 2024b; Jia et al., 2025). In MAR, the authors model the per-token probability distribution with a diffusion model (in the form of a small MLP) conditioned on a latent variable modeled by an autoregressive transformer backbone.

SALAD (Turetzky et al., 2024) and DiTAR (Jia et al., 2025) adapt MAR-style diffusion heads for text-to-speech modeling, achieving better audio quality than discrete baselines. However, these works are limited to text-to-speech on small-scale and domain-specific datasets, leaving open the question of how well they can adapt to richer audio domains such as music.

In this work, we propose Continuous Audio Language Models (CALM) that predict sequences in the latent space of a VAE, bypassing the need for quantization. While we build on the MAR architecture where a transformer backbone uses $(\mathbf{x}^1, \ldots, \mathbf{x}^{s-1})$ to predict an intermediate latent $\mathbf{z}^s$, which then conditions a head (diffusion model) that models $p(\mathbf{x}^s | \mathbf{z}^s)$, we find that without further improvements, it fails to generate rich audio content. To overcome this, we introduce several key innovations:

1. Improving quality and stability: To mitigate error accumulation during inference, we follow Pasini et al. (2024b) and, during training, inject noise into the long-term context $(\mathbf{x}^1, \ldots, \mathbf{x}^{s-1})$. Additionally, we introduce a short-context transformer that summarizes recent clean latents, providing the sampling head with both coarse long-range context and fine-grained local information.
2. Diffusion-to-Consistency replacement: We replace the diffusion model with a continuous consistency model (Lu & Song, 2025) during training, significantly accelerating inference without compromising sample quality. This change reduces the inference time of the sampler head by a factor of up to $\times 20$ in our music experiments and $\times 12$ in our speech experiments compared to the use of a model that uses an RQ-Transformer as head. This method is modality-agnostic and may benefit other domains such as image generation. **3. Gaussian Temperature sampling**: Temperature control is crucial for high-quality speech generation, yet consistency models lack a formal mechanism for temperature sampling. We present a heuristic that approximates temperature sampling in the consistency setup. **4. Head batch multiplier**: Sampling multiple noise levels at training time for the same latent highly accelerates training for a small cost.

Our model generates high-quality speech and music with lower inference time, outperforming state-of-the-art discrete-token autoregressive models in both efficiency and audio fidelity. To our knowledge, this is the first application of autoregressive continuous latent modeling to both domains.

2 Related Work

Autoregressive audio language models. Early autoregressive audio models operated on raw waveforms such as WaveNet (van den Oord et al., 2016) or learned discrete codes via VQ-VAE, such as in Jukebox (Dhariwal et al., 2020). The advent of neural audio codecs (Zeghidour et al., 2021; Défossez et al., 2024a) enabled high-quality vector-quantized tokenizers for general audio. These, in turn, powered discrete-token audio LMs: AudioLM (Borsos et al., 2023) for unconditioned audio generation while AudioGen (Kreuk et al., 2023), MusicLM (Agostinelli et al., 2023), and MusicGen (Copet et al., 2023) apply similar methods for text-to-audio and text-to-music generation. In speech, autoregressive modeling of RVQ codes has been used for text-to-speech generation (Wang et al., 2023; Kharitonov et al., 2023) as well as for spoken dialogue (Défossez et al., 2024b) or translation (Labiausse et al., 2025). However, all of these systems rely on lossy quantization, which inevitably degrades audio fidelity unless a significant compute budget is spent to generate a deep hierarchy
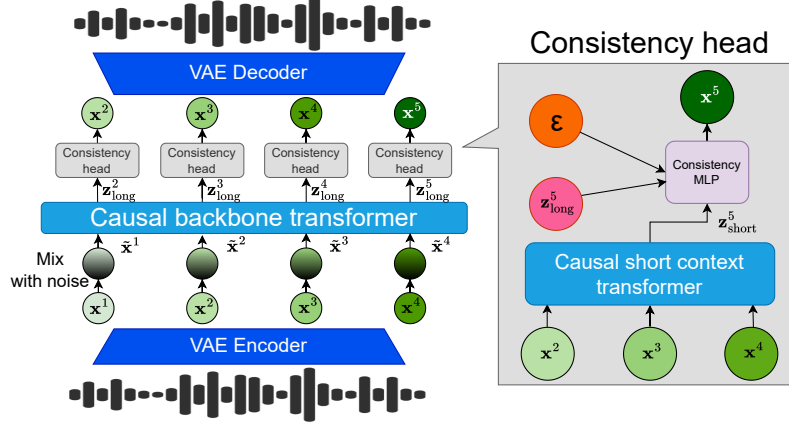
Figure 1: Overview of our model. During training, latent vectors $\mathbf{x}^s$ are noised to encourage the backbone Transformer to focus on coarse structure. The consistency head is a consistency model conditioned on the latent variable $\mathbf{z}^{\mathbf{s}}_{\text{long}}$ produced by the backbone, as well as a short-term context vector $\mathbf{z}^{\mathbf{s}}_{\text{short}}$ computed from a short-context Transformer applied to the most recent clean latent tokens.

of RVQ tokens. This is unlike CALM, which predicts continuous embeddings in one pass, providing a better quality-computation trade-off.

Continuous autoregressive models. In GIVT, Tschannen et al. (2024) use a transformer to autoregressively model the latent space of a VAE trained on images, parameterize a Gaussian Mixture Model, and train it with a cross-entropy loss. The authors of MAR (Li et al., 2024) obtain better results by replacing the Gaussian mixture model with a diffusion-model enabling the approximation of more flexible distributions. In MAR, a large transformer backbone predicts a continuous embedding $\mathbf{z}^s$ given $(\mathbf{x}^1, \ldots, \mathbf{x}^{s-1})$, which then conditions a small MLP diffusion network that models the probability distribution $p(\mathbf{x}^s|\mathbf{z}^s)$ of the next latent. This eliminates the need for discrete tokenizers, but at the cost of slow sampling: MAR typically needs hundreds of denoising steps per token. Hang et al. (2025) aims to speed up MAR by replacing the diffusion head with a shortcut head (Frans et al., 2025) for few-step sampling. Shortcut models combine a diffusion loss and a self-consistency loss in order to accelerate the diffusion process. They reduce the number of diffusion steps from 100 to 8 with a similar image quality. Apart from this work, we are not aware of other works that try to reduce the inference time of the diffusion process in continuous autoregressive models. Remarkably, CALM achieves a quality comparable to the best discrete models with only one step of consistency modeling.

In audio, the approach of MAR has been adapted for the task of Text-to-Speech (TTS) synthesis. SALAD (Turetzky et al., 2024) introduces a zero-shot TTS model that operates on continuous speech representations using a per-token latent diffusion process. By leveraging semantic tokens for contextual information and determining synthesis stopping points, SALAD achieves improved intelligibility and audio quality without relying on quantization. Similarly, DiTAR (Jia et al., 2025) presents a patch-based autoregressive framework combining a language model with a diffusion transformer for speech generation. This approach models dependencies between aggregated local patches of continuous tokens, using a causal language model to produce embeddings, which, along with previous patches, serve as inputs to a bidirectional diffusion transformer that predicts the next patch. The authors observe that providing local context through patching was determinant to improve their model, which corroborates what we observe with the introduction of a short context transformer into our model. While these two studies focus on TTS modeling, we extend the method to music. In Pasini et al. (2024b), the authors apply the MAR framework to music generation using a relatively small dataset comprising 20,000 single-instrument stems, training their model on 10-second excerpts on top of their continuous compression model Music2Latent (Pasini et al., 2024a). They introduce a method for noise augmentation of the data that allows the model to avoid error accumulation. However, we notice that scaling to a more complex and diverse dataset consisting of full musical pieces makes their approach struggle to maintain high-quality generation on longer sequences. To address these challenges, we propose novel strategies that enhance generation quality while also improving inference efficiency. Finally, Music2Latent2 (Pasini et al., 2025) explores combining autoregressive and consistency modeling but for compression.

3 Background

Notations: Let $W \in \mathbb{R}^{f_s \cdot d}$ be a monophonic waveform of d seconds sampled at frame rate f_s. Our goal is to model W either in the discrete latent space of a RVQ-based codec or in the latent space of a VAE. Let f_r be the frame rate of the codec or VAE.

In the case of the **discrete modeling**, W is represented by the sequence of discrete tokens $(q^{s,k})$, where $s \in \{1, \ldots, S\}$ indexes time and $k \in \{1, \ldots, K\}$ indexes codebook depth and $S = f_r \cdot d$. Each token $q^{s,k} \in \{1, \ldots, N_k\}$ is drawn from a finite vocabulary.

In the case of **continuous modeling**, W is represented by a sequence $(\mathbf{x}^1, \ldots, \mathbf{x}^S)$ with $S = f_r \cdot d$ and $\mathbf{x}^s \in \mathbb{R}^C$ where C is the latent dimension of the VAE.

3.1 Autoregressive Modeling with Residual Vector Quantization based codecs.

Autoregressive modeling of discrete tokens from RVQ-based codecs (Zeghidour et al., 2021; Défossez et al., 2024a) is a prevalent method for high-fidelity audio generation (Copet et al., 2023; Agostinelli et al., 2023; Borsos et al., 2023; Kreuk et al., 2023). Given a sequence of discrete tokens $\left(q^{s,k}\right)_{i \in \{1, \ldots, N\}, k \in \{1, \ldots, K\}}$, early models like Borsos et al. (2023); Agostinelli et al. (2023) flattened the multi-level sequence, increasing its length by a factor of K and resulting in high computational costs due to the quadratic complexity of Transformer self-attention. MusicGen (Copet et al., 2023) mitigates this by using a delay pattern to independently sample each of the K RVQ levels, adding only $K - 1$ tokens to the sequence but introducing a fixed latency of $K - 1$ frames, which is problematic for real-time applications. RQ-Transformer (Lee et al., 2022) addresses this by using a sampler transformer head that models the RVQ at a given time step, enabling low-latency generation.

Denoting $\mathbf{q}^s = (q^{s,1}, \ldots, q^{s,K})$, the *Backbone Transformer* T_θ encodes the history of previous timesteps to produce a context vector $\mathbf{z}^s$, and a *RQ-Transformer* g_ϕ autoregressively decodes the residual-wise components of the token stack at each time step. The context vector is then given by $\mathbf{z}^s = T_\theta(\mathbf{q}^1, \ldots, \mathbf{q}^{s-1})$, and the logits $\ell^{s,k}$ for predicting the k-th codebook token are computed as $\ell^{s,1} = \mathrm{Lin}(\mathbf{z}^s)$ and $\ell^{s,k} = g_\phi\left(\mathbf{z}^s, q^{s,1}, \ldots, q^{s,k-1}\right)$ for $k > 1$.

These logits are trained using a cross-entropy loss over discrete tokens $\mathcal{L}_{\mathrm{CE}} = -\sum_{s=1}^{S} \sum_{k=1}^{K} \log p\left(q^{s,k} \mid \mathbf{q}^{<s}, \mathbf{q}^{s,<k}\right)$.

This approach enables efficient parallel modeling of RVQ sequences, allowing all codebooks corresponding to a single timestep to be generated simultaneously without introducing any delay. However, a key limitation lies in the use of the *RQ-Transformer*, which is computationally intensive; as its resource requirements scale with the number of RVQ.

3.2 Consistency Models

Flow Matching and Probability Flow ODE. Let p_{data} be a data distribution over $\mathbb{R}^d$. Given $\mathbf{x}_0 \sim p_{\mathrm{data}}$, diffusion (Ho et al., 2020; Song et al., 2021) and flow matching (Lipman et al., 2023) models define a forward noising process that gradually perturbs samples from p_{data} through the noising process $\mathbf{x}_t = \alpha_t \mathbf{x}_0 + \sigma_t \boldsymbol{\epsilon}$, where $\boldsymbol{\epsilon} \sim \mathcal{N}(0, \mathbf{I})$ and $t \in [0, T]$. α_t, σ_t are pre-defined functions such that α is decreasing with $\alpha_0 = 1, \alpha_T = 0$ and σ is increasing with $\sigma_0 = 0, \sigma_T = 1$. In Flow Matching, a neural network F_ϕ is trained to minimize the loss

$$\mathcal{L}_{\mathrm{FM}}(\phi) = \mathbb{E}_{\mathbf{x}_0 \sim p_{\mathrm{data}}, \, \boldsymbol{\epsilon} \sim \mathcal{N}(0, \mathbf{I}), \, t \sim \mathcal{U}(0,1)} \left[w(t) \left\| F_\phi(\mathbf{x}_t, t) - (\alpha'_t \mathbf{x}_0 + \sigma'_t \boldsymbol{\epsilon}) \right\|_2^2 \right].$$

Once trained, sample generation is performed by solving a deterministic ordinary differential equation known as the probability flow ODE (PF-ODE), which defines a continuous path from noise to data. In the context of Flow Matching, the PF-ODE is $\frac{d\mathbf{x}_t}{dt} = F_\phi(\mathbf{x}_t, t)$ with $\mathbf{x}_T \sim \mathcal{N}(0, \mathbf{I})$.

A **Continuous-Time Consistency Models.** (Song et al., 2023) is a neural network $f_\phi(\mathbf{x}_t, t)$ trained to map a noisy input $\mathbf{x}_t$ directly to the corresponding clean data $\mathbf{x}_0$ in a single step, by approximating the sampling trajectory of the probability flow ODE (PF-ODE) starting from $\mathbf{x}_t$. To ensure correct behavior, f_ϕ must satisfy the boundary condition $f_\phi(\mathbf{x}, 0) = \mathbf{x}$, thus leading to the common parameterization $f_\phi(\mathbf{x}_t, t) = c_{\mathrm{skip}}(t)\mathbf{x}_t + c_{\mathrm{out}}(t)F_\phi(\mathbf{x}_t, t)$, where F_ϕ is a neural network and the coefficients satisfy $c_{\mathrm{skip}}(0) = 1$ and $c_{\mathrm{out}}(0) = 0$ to fulfill the boundary condition.

By using $T = \frac{\pi}{2}$ and $\alpha_t = \cos(t), \sigma_t = \sin(t)$, Lu & Song (2025) derive the following continuous-time consistency loss where $w_\psi(t)$ is an adaptive weighting function:

$$\mathcal{L}_{\text{CM}}(\phi, \psi) = \mathbb{E}_{\mathbf{x}_t, t} \left[\frac{e^{w_\psi(t)}}{D} \left\| F_\phi(\mathbf{x}_t, t) - F_{\phi^-}(\mathbf{x}_t, t) - \cos(t) \frac{df_{\phi^-}(\mathbf{x}_t, t)}{dt} \right\|_2^2 - w_\psi(t) \right]. \quad (1)$$

3.3 Autoregressive Modeling of Continuous Latents via Diffusion.

Li et al. (2024) propose MAR, a method for autoregressive modeling over a sequence $(\mathbf{x}^1, \dots, \mathbf{x}^S)$ of continuous latent vectors extracted from a pretrained VAE, thereby eliminating the need for discrete quantization. As in the discrete case, a *Backbone Transformer T_θ* maps the context to an embedding: $\mathbf{z}^s = T_\theta(\mathbf{x}^1, \dots, \mathbf{x}^{s-1})$.

Then, a diffusion process parameterized by a neural network ϵ_ϕ is trained on each $\mathbf{x}^s$ with the loss $\mathcal{L}_{\text{diff}}(\theta, \phi) = \sum_{s=1}^S \mathbb{E}_{\epsilon \sim \mathcal{N}(0, I), t \sim [0,1]} \left[\|\epsilon - \epsilon_\phi(\mathbf{x}_t^s, \mathbf{z}^s, t)\|^2 \right]$ where $\mathbf{x}_t^s$ is a noisy version of $\mathbf{x}^s$ at diffusion timestep t: $\mathbf{x}_t^s = \alpha_t \mathbf{x}^s + \sigma_t \epsilon$ with $\epsilon \sim \mathcal{N}(0, I)$ and α_t and σ_t are predefined schedules for all $t \in [0, 1]$. In practice, an MLP significantly smaller than the backbone transformer estimates ϵ_ϕ. This replaces the categorical prediction used in discrete models (done by the RQ-Transformer) with a denoising task in the continuous domain (done by the MLP). This method enables flexible and differentiable modeling of continuous signals without requiring to perform quantization on the latent space which can lead to several issues such as codebook collapse, balancing quantization losses and training instabilities. A key limitation of this approach is that sample quality depends on the number of diffusion steps at inference, raising the question of whether it can surpass the RQ-Transformer under similar computational constraints.

4 Method

4.1 Our VAE-GAN

Most autoregressive audio models are built upon RVQ-GAN architectures (Zeghidour et al., 2021; Défossez et al., 2024a; Kumar et al., 2023; Guo et al., 2025). Following the approach of Evans et al. (2024), we instead adopt a VAE-GAN framework, replacing the RVQ bottleneck with a VAE bottleneck to regularize the latent space and enforce a Gaussian prior. Our VAE is fully causal and draws from the architecture of Mimi (Défossez et al., 2024b), using Transformers in addition to convolutions in the encoder and decoder, which have been shown to improve performance.

While training the model with adversarial losses and VAE regularization without any reconstruction losses improves the quality of the model for speech, it degrades the reconstruction quality for music. Semantic distillation is performed for the speech VAE similarly as in Mimi, with WavLM (Chen et al., 2021) as teacher. There is no semantic distillation for the music model and we let this for future work as semantic content is harder to define for music. The loss is:

$$\mathcal{L}_{\text{VAE}} = \lambda_t \mathcal{L}_t(x, \hat{x}) + \lambda_f \mathcal{L}_f(x, \hat{x}) + \lambda_{\text{adv}} \mathcal{L}_{\text{adv}}(\hat{x}) + \lambda_{\text{feat}} \mathcal{L}_{\text{feat}}(x, \hat{x}) + \lambda_{\text{KL}} \mathcal{L}_{\text{KL}} \quad (2)$$

where $\mathcal{L}_t$ and $\mathcal{L}_f$ are the temporal and frequential reconstruction losses, $\mathcal{L}_{\text{adv}}$ is the adversarial loss, $\mathcal{L}_{\text{feat}}$ is the feature matching loss and $\mathcal{L}_{\text{KL}}$ is the KL regularization applied to the VAE bottleneck.

4.2 Consistency-Based Continuous Audio Language Model (CALM)

Let $(\mathbf{x}^1, \dots, \mathbf{x}^S)$ denote the sequence of continuous latent vectors produced by a VAE encoder. As illustrated in Fig. 1, our model comprises three main components:

1. Causal Backbone Transformer with Noise Injection　We build on the MAR framework (Li et al., 2024) by employing a causal Transformer $T_{\text{long}, \theta^1}$ to capture long-term dependencies. During training, each input latent $\mathbf{x}^s$ is replaced with a noised version $\tilde{\mathbf{x}}^s$ (see Sec. 4.3 and Ablation 5). We don't perform any noise augmentation at inference time. Concretely, $\mathbf{z}_{\text{long}}^s = T_{\text{long}, \theta^1}(\tilde{\mathbf{x}}^1, \dots, \tilde{\mathbf{x}}^{s-1})$. Noise injection prevents error accumulation during inference, but as shown in Tab. 5 is insufficient alone for high-quality music generation.

2. Short-Context Transformer   To supply local, high-resolution context to the denoising head, we introduce a lightweight causal Transformer that attends the K previous clean latents (we use $K = 10, \sim 0.4s$ of music): $\mathbf{z}_{\text{short}}^s = T_{\text{short},\theta^2}\left(\mathbf{x}^{s-K}, \ldots, \mathbf{x}^{s-1}\right)$. This short-context embedding $\mathbf{z}_{\text{short}}^s$ supplies fine-grained information potentially lost through noise injection in the backbone. We show in Tab. 7 that the value of K is not a decisive hyperparameter.

3. Consistency-Model Head   Finally, a small MLP-based consistency model f_ϕ is conditioned on the sum of the long-term and short-term features, $\mathbf{Z}^s = \mathbf{z}_{\text{long}}^s + \mathbf{z}_{\text{short}}^s$. At inference time, for 1-step, the next latent $\hat{\mathbf{x}}^s$ is sampled through: $\boldsymbol{\epsilon} \sim \mathcal{N}(0, I), t = 1, \hat{\mathbf{x}}^s = f_\phi\left(\mathbf{x}_1^s = \boldsymbol{\epsilon}, t = 1, \mathbf{Z}^s\right)$.

In addition to consistency, we experiment with the TrigFlow (Lu & Song, 2025) formulation of flow-matching for the MLP. Although TrigFlow yields marginally higher fidelity, its inference cost makes it impractical for real-time use. This tradeoff is studied in Sec. 5.2, Tab. 4.

Together, these three components form a continuous autoregressive model that (i) leverages noise-robust long-term modeling, (ii) preserves local detail via short-context conditioning, and (iii) achieves rapid, high-fidelity latent sampling through consistency modeling.

The training objective for one sequence $\left(\mathbf{x}^1, \ldots, \mathbf{x}^S\right)$ is defined by:

$$\mathcal{L}_{\text{CALM}}(\theta, \phi, \psi) = \sum_{s=1}^{S} \mathbb{E}_{t,\epsilon} \left[\frac{e^{w_\psi(t)}}{D} \left\| F_\phi\left(\mathbf{x}_t^s, t, \mathbf{Z}^s\right) - F_{\bar{\phi}}\left(\mathbf{x}_t^s, t, \mathbf{Z}^s\right) - \cos(t) \frac{df_{\bar{\phi}}(\mathbf{x}_t^s, t, \mathbf{Z}^s)}{dt} \right\|_2^2 - w_\psi(t) \right],$$

$$(3)$$

where $\mathbf{Z}^s = \mathbf{z}_{\text{long}}^s + \mathbf{z}_{\text{short}}^s = T_{\text{long},\theta^1}\left(\tilde{\mathbf{x}}^1, \ldots, \tilde{\mathbf{x}}^{s-1}\right) + T_{\text{short},\theta^2}\left(\mathbf{x}^{s-K}, \ldots, \mathbf{x}^{s-1}\right)$, $t \sim [0, 1], \boldsymbol{\epsilon} \sim \mathcal{N}(0, I)$ and $\mathbf{x}_t^s = \cos(t)\mathbf{x}^s + \sin(t)\boldsymbol{\epsilon}$. All the parameters (θ, ϕ, ψ) of the transformer backbone T_{long,θ^1}, the short-context transformer $T_{\text{short},\theta^2}$, the consistency MLP f_ϕ and the adaptive weighting function w_ψ are jointly trained together with this consistency loss similarly as the backbone and the RQ-Transformer are trained through cross-entropy loss in the discrete case.

4.3   Combining noisy long-term context and clean short-term context

In preliminary experiments, we realized that the music generation model was diverging quite quickly during inference because it was not robust to error accumulation. Pasini et al. (2024b) introduce a noise augmentation trick at training time in order to tackle this problem. Given a sequence $(\mathbf{x}^1, \mathbf{x}^2, \ldots, \mathbf{x}^S)$, they sample $k_s \sim \mathcal{U}(0, 1)$ and $\boldsymbol{\epsilon}_s \sim \mathcal{N}(0, \mathbf{I})$ for every $s \in \{1, \ldots, S\}$ and compute $\tilde{\mathbf{x}}^s = k_s \boldsymbol{\epsilon}_s + (1 - k_s)\mathbf{x}^s$ for every s. After comparison and to preserve the variance of the $\mathbf{x}^s$ that are gaussians, we modify the noising formula as follows: $\tilde{\mathbf{x}}^s = \sqrt{k_s}\boldsymbol{\epsilon}_s + \sqrt{1 - k_s}\mathbf{x}^s$

In our case, applying this noising method to music generation slightly improves model stability but often reduces detail and instrument diversity, typically preserving only rhythmic elements, with audio fading into silence after 10–15 seconds. Since Pasini et al. (2024b) targets short, single-instrument clips, it's unsurprising the method performs best in that constrained setting. We hypothesize that the added noise inhibits the backbone transformer from encoding fine-grained information into $\mathbf{z}_{\text{long}}^s$, limiting the MLP's ability to reconstruct detailed audio. However, combining this with a short-context transformer computing $\mathbf{z}_{\text{short}}^s$ yields the best results (Tab. 5), likely because the clean short-term context restores local detail needed to model the distribution of the next $\mathbf{x}^s$.

At inference time, we omit noise augmentation and achieve our best results with this setup. Providing historical context to the diffusion head was used in the TTS model DiTAR (Jia et al., 2025), which reported a significant reduction in word error rate when using it.

4.4   Head Batch Multiplier

Training is bottlenecked by the cost of generating the conditioning variable $\mathbf{z}_{\text{long}}^s$ via the large causal transformer. To address this, we introduce the *Head Batch Multiplier*, which amortizes this cost by reusing $\mathbf{z}_{\text{long}}^s$ multiple times per training step. Specifically, for each input sequence, we compute $\mathbf{z}_{\text{long}}^s$ once and use it across N loss computations, each with independently sampled noise levels t and ϵ. This not only improves efficiency but also stabilizes training by averaging the loss over multiple

Table 1: **Speech compression models.** Our VAE is on par with the VQ-VAE on acoustic quality (MOSNeT) and outperforms it on semantic discriminability (ABX).

MODEL TYPE	DIMS / RVQ	FRAME RATE (Hz)	BITRATE (KBIT/S)	MOSNET (↑)	ABX (↓)
VQ-VAE (MIMI)	8 RVQ	12.5	1.1KBPS	3.11	9.4%
VAE	32 DIMS	12.5	-	**3.15**	**8.1%**

samples. As shown in Tab. 5 and Fig. 2, this leads to faster convergence and better final performance at comparable training cost.

4.5 Gaussian temperature sampling

Sampling strategies, such as temperature sampling, have a significant impact on generation quality in the discrete setup, particularly for speech. To replicate this behavior in the continuous domain, we introduce a sampling heuristic that results in similar gains.

Let $\epsilon \sim \mathcal{N}(0, I)$ be a standard multivariate Gaussian random variable and let $\mathbf{x} = f(\epsilon)$, where $f : \mathbb{R}^d \to \mathbb{R}^d$ is a differentiable function. By the change of variables formula, the probability density of $\mathbf{x}$ is given by: $p(\mathbf{x}) = p(\epsilon) \cdot \left| \det \left(\frac{\partial f(\epsilon)}{\partial \epsilon} \right) \right|^{-1}$, where $\frac{\partial f(\epsilon)}{\partial \epsilon}$ is the Jacobian matrix of f at ϵ. In theory, to apply temperature sampling with temperature τ we should raise both terms to the power $1/\tau$, but the Jacobian term is untractable. In practice, we noticed that we can apply temperature only on the Gaussian noise sampling (which is equivalent to sampling from a Gaussian with variance $1/\sqrt{\tau}$) and get significant improvements in metrics.

The effects of gaussian temperature are further discussed in Section 5.3.

5 Experiments and results

We now present experimental results on both speech and music continuation. We generate 27 seconds following a prompt of 3 seconds. All detailed hyperparameters are in the Appendix Sec. C. All metrics reported with confidence intervals use 95% confidence. Metrics without confidence intervals are metrics computed over the entire test dataset.

5.1 Speech Continuation

VAE: Our VAE is based on Mimi (Défossez et al., 2024b) but enforces gaussian inner latents instead of a categorical distribution. Like in Mimi, to enforce semanticity of the representations, we distill WavLM into the inner latent representation with a cosine similarity loss. Unlike Mimi, which applies this loss only to the first codebook, we extend it to the entire latent representation.

Model and dataset: Starting from Helium-1 (Kyutai, 2025), a pretrained 2B parameters multilingual text LM as backbone, we train on French and English speech data following Défossez et al. (2024b) to learn continuation. To enhance the stability and coherence of speech continuation, we adopt the concept of *inner monologue* (Défossez et al., 2024b)—a latent textual representation of the model's own speech, aligned such that each word is positioned at the timestep corresponding to its spoken occurrence. This implies that, at each timestep s, the backbone transformer takes both text tokens and speech latents as input, and that its output $\mathbf{z}_{\text{long}}^s$ is passed through a linear layer which produces text logits alongside conditioning the consistency head. This internal text stream acts as a semantic scaffold, as it represents the next word to be pronounced, guiding the generation of audio tokens by grounding them in a linguistic form. Crucially, like in Défossez et al. (2024b), we introduce a temporal delay of 2 time steps (160ms) between the inner monologue and the corresponding audio tokens. This delay allows the model to access textual content prior to generating acoustic latents, decoupling high-level planning from low-level synthesis. For speech generation, we didn't notice any gains from introducing a short context transformer and noising the latents before feeding them to the backbone, resulting in a simpler model architecture.

Results: Tab. 1 shows that our 32-dimensional VAE matches an 8-RVQ Mimi codec on MOSNet (Lo et al., 2019), which measures audio quality, and exceeds it on the ABX metric (Schatz et al.,

2013). ABX evaluates phonetic discriminability by testing whether a word like "bat" is represented closer to another "bat" utterance than to a similar-sounding word like "bit", based on latent distances.

Tab. 2 shows that the 1-step Consistency model outperforms the RQ-Transformer with 8 RVQ on all our automatic and human based metrics as well as on speed. For automatic metrics, we compute PPX and VERT Lakhotia et al. (2021). The PPX metric measures the semantic meaningfulness of the generated speech. To do so we generate 1000 excerpts of speech of 30 second, we use Whisper Radford et al. (2022) to compute textual transcriptions and finally compute the negative log-likelihood of the text tokens with a Mistral 7B LLM Jiang et al. (2023) and convert it to Perplexity. Because a model that generates poorly diverse but good quality sentences would perform well on the PPX metric, the authors of Lakhotia et al. (2021) introduce the VERT metric (for diVERsiTy) which is a geometric mean of self- and auto-BLEU metrics. We use the official implementation from the fairseq Ott et al. (2019) repository.

To assess perceptual quality, we conduct two human evaluation studies involving 50 participants and 50 randomly selected examples from the English test set. Each participant rates 10 examples across the following evaluation protocols: For Acoustic Quality, participants are presented with all model continuations for the same prompt, including the ground truth reference, and rate the acoustic quality of each continuation on a 1 to 5 scale. For Meaningfulness, participants are shown two continuations of the same prompt and select the one that is the most meaningful. These pairwise preferences are used to compute an Elo score (see Sec. B).

Notably, we note a clear quality and meaningfulness improvement with our temperature method. Given that there is a text stream to guide the audio generation, we expected the CALM to match the baseline on meaningfulness rather than outperforming it. This phenomenon could be due to less model capacity in the backbone being allocated to audio manipulation, allowing more for text prediction. On the inference speed side, the consistency head is $\times 12.3$ faster than the RQ-Transformer. The overall gain to perform a full inference of 30 seconds is $\times 1.3$.

Table 2: **Comparison of speech continuation models**: 8-RVQ RQ-transformer vs 1-step Consistency model head, with 2 temperature options.

Model Type	Sampling temperature	Overall Speedup (↑)	Sampler Speedup (↑)	% Time in Sampler (↓)	PPX (↓)	VERT (↓)	Acoustic Quality(↑)	Meaningfulness Elo (↑)	Rank (↓)
Reference	–	–	–	–	20.2 ± 0.1	25.2 ± 0.1	4.02 ± 0.11	2180 ± 30	–
RQ-transformer 8 RVQ	1.0	$\times 1.0$	$\times 1.0$	26.7%	52.4 ± 0.2	36.3 ± 0.2	2.42 ± 0.12	1841 ± 25	4
RQ-transformer 8 RVQ	0.8	$\times 1.0$	$\times 1.0$	26.7%	26.8 ± 0.1	33.1 ± 0.1	2.75 ± 0.14	1870 ± 30	3
CALM - Consistency - 1 step	1.0	$\times 1.3$	$\times 12.3$	2.9%	42.9 ± 0.2	34.3 ± 0.2	2.82 ± 0.13	1947 ± 28	2
CALM - Consistency - 1 step	0.8	$\times 1.3$	$\times 12.3$	2.9%	$\mathbf{23.8 \pm 0.1}$	$\mathbf{31.2 \pm 0.1}$	$\mathbf{3.45 \pm 0.14}$	$\mathbf{2023 \pm 27}$	**1**

5.2 Music Continuation

Dataset: We use a randomly selected subset of 400K songs (approximately 20K hours with 32kHz mono format) from the LAION-Disco-12M dataset, ensuring broad coverage across musical genres.

VAE: Our variational autoencoder (VAE) and codec architecture are adapted from the Mimi codec (Défossez et al., 2024b), originally designed for 24kHz speech at 12.5Hz. We trained it to compress 32kHz mono music with a 25Hz frame rate. We experiment with bottleneck sizes of 96 and 128 dimensions. For comparison, MusicGen's EnCodec model (Copet et al., 2023) also operates at 32kHz but uses a 4-level RVQ at 50Hz. In Tab. 3, we report reconstruction metrics (audio ViSQOL Chinen et al. (2020) and SISNR), showing that a 32-dim VAE matches MusicGen's codec, and that at least 96 dimensions are needed for our VAE to match the quality of the 32-level RVQ configuration.

Table 3: **Music compression models.** At least 96 VAE latent dimensions are required to outperform the 32-RVQ codec on reconstruction metrics. EnCodec has been retrained on our dataset.

MODEL TYPE	DIMS / RVQ	FRAME RATE (HZ)	BITRATE (KBPS)	VISQOL (↑)	SISNR (↑)
ENCODEC COPET ET AL. (2023)	4 RVQ	50	2.2	2.41	5.62
VQ-VAE (INSPIRED FROM MIMI)	32 RVQ	25	8.8	3.63	9.61
VAE	32 DIMS	25	–	2.23	5.51
VAE	96 DIMS	25	–	3.65	9.76
VAE	128 DIMS	25	–	**4.01**	**10.3**

Table 4: **Comparison of music generation models across speed and quality metrics for 30 seconds generation.** Consistency-based models provide up to a $2.2\times$ overall speedup and a $19.3\times$ sampler head speedup compared to the RQ-Transformer 32 RVQ baseline, while achieving improved FAD scores and equivalent human ratings. TrigFlow achieves the best qualitative results but has significantly higher inference time. Since MusicGen only uses a linear layer to sample its token we consider its inference cost as negligible.

MODEL	OVERALL SPEEDUP ($\uparrow$)	SAMPLER SPEEDUP ($\uparrow$)	% TIME IN SAMPLER ($\downarrow$)	FAD ($\downarrow$)	ACOUSTIC QUALITY ($\uparrow$)	ENJOYMENT ELO ($\uparrow$)	RANK ($\downarrow$)
REFERENCE	–	–	–	–	3.84 ± 0.08	2166 ± 33	-
RQ-TRANSFORMER 32 RVQ (BASELINE)	$\times 1.0$	$\times 1.0$	57.7%	1.06 ± 0.06	2.85 ± 0.07	1824 ± 29	4
RQ-TRANSFORMER 16 RVQ	$\times 1.5$	$\times 2.2$	38.0%	1.43 ± 0.07	2.76 ± 0.07	1781 ± 29	5
CALM - CONSISTENCY - 1 STEP	$\times \mathbf{2.2}$	$\times \mathbf{19.3}$	**6.6%**	0.83 ± 0.04	2.90 ± 0.07	1857 ± 28	2
CALM - CONSISTENCY - 4 STEPS	$\times 1.9$	$\times 5.4$	20.1%	$\mathbf{0.71 \pm 0.05}$	3.07 ± 0.07	1847 ± 24	3
CALM - TRIGFLOW - 100 STEPS	$\times 0.3$	$\times 0.2$	86.6%	$\mathbf{0.64 \pm 0.04}$	3.12 ± 0.07	$\mathbf{1921 \pm 29}$	**1**
MUSICGEN MEDIUM	$\times 1.3$	–	0.0%	1.72 ± 0.12	2.62 ± 0.07	1761 ± 33	6

MODEL VARIANT	FAD ($\downarrow$)
BASE (CALM - CONSISTENCY - 4 STEPS)	$\mathbf{0.93 \pm 0.06}$
W/O HEAD BATCH MULTIPLIER	1.32 ± 0.09
W/O NOISE AUGMENTATION	1.63 ± 0.11
W/O SHORT CONTEXT TRANSFORMER	4.03 ± 0.16
W/O ANY OF THE ABOVE	8.38 ± 0.17

Table 5: **Ablation study on music CALM Consistency 4-steps model components, after 250K training steps.** Removing noise augmentation or the short-context transformer leads to significant performance drops. Final row approximates the MAR configuration from Li et al. (2024).

Model: Our music CALM builds on the MusicGen Medium backbone, a 1.35B parameter Transformer (see Sec. C for all the hyperparameters). We compare our method against: (1) Two discrete models using 32 and 16 RVQ codecs, each employing the same 1.35B backbone and a RQ-transformer for parallel codes prediction; (2) a MusicGen Medium variant trained with EnCodec without textual conditioning, using the same backbone and a delay pattern for codebook interleaving. Both MusicGen Medium and EnCodec models were trained on our dataset.

Results and Ablation: In Tab. 4, we report both objective metrics and the results of a human evaluation study for the task of music continuation, conditioned on a 3-second prompt. We compute the speed-up compared to the RQ-Transformer 32 RVQ, the Fréchet Audio Distance (FAD) which is the distance between Gaussian distributions fitted on VGG-obtained embeddings of the real and generated samples. We compute it on 4,000 model-generated continuations from the test set. The Acoustic Quality is a MOS score between 1 and 5. The Enjoyment metric is an Elo score (see Sec. B), computed by making human rater choose their favorite music out of generated pairs with the same 3s prompt. The evaluation protocol uses the same amount of annotators and examples as the speech study. We observe that CALM with consistency outperforms the 32 RVQ RQ-Transformer baseline on computed and human metrics while being $\times 1.9$ to $\times 2.2$ times faster for the overall speedup. While the RQ-Transformer takes 57.7% of the inference time for the baseline, the consistency head only takes 6.6% to 20.1%. As well, we train a CALM model with a TrigFlow head instead of consistency and it outperforms all the models but to the price of a slow inference.
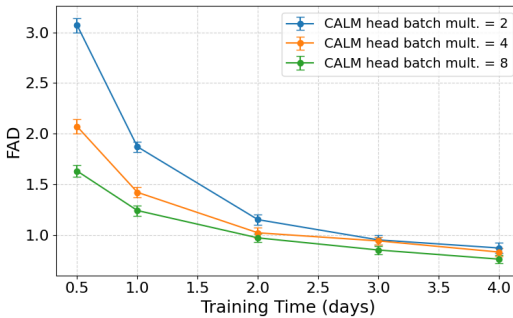

Figure 2: **Effect of the head batch multiplier value.** Training a model (music consistency CALM) with a higher batch size multiplier fastens the convergence for the FAD metric. All the evaluations are done with 4 steps of consistency at inference time.

An ablation study (Tab. 5) on music CALM Consistency 4 steps shows the importance of each component. The experiments are run for 250K steps, which explains that the base model's FAD is worse than the one reported in Tab. 4. The final row that is the closest to the MAR framework

(consistency replacing diffusion) fails to produce high-quality music. In Fig. 2, we show that the FAD decreases much faster over time when we train consistency CALM models with a bigger head batch multiplier. All evaluations are done with 4 steps of consistency. We keep the value of 8 for all of our experiments as a higher value would lead to out of memory issues at training time.

Scalability: We show in Sec. A.2 that CALM does improve with a bigger 3B parameters backbone. However, we leave a complete scalability study for future work.

Necessity of Consistency for a fast inference: We show in Tab. 6 that the consistency framework largely outperforms the TrigFlow framework for 10 inference steps and less (the regime where the Real time factor is greater than 1).

# STEPS	TIME (S)	RTF	FAD (TRIGFLOW)	FAD (CONSISTENCY)
1	16.7	×1.80	–	0.83 ± 0.04
4	20.4	×1.47	28.83 ± 0.20	0.71 ± 0.05
10	27.7	×1.08	4.62 ± 0.07	0.73 ± 0.05
25	46.1	×0.65	0.79 ± 0.04	0.96 ± 0.06
50	76.8	×0.39	0.74 ± 0.05	1.46 ± 0.06
100	136.4	×0.22	0.64 ± 0.04	2.05 ± 0.07

Table 6: **Generation efficiency of TrigFlow CALM and Consistency CALM models.** We compute the inference time to generate 30 seconds of audio, the corresponding Real Time Factor (RTF) as well as the FAD metric for different numbers of inference steps. For less than 10 steps (i.e. when streaming applications are possible, the consistency method outperforms the TrigFlow method).

5.3 Effect of gaussian temperature sampling

We evaluate how our proposed gaussian temperature sampling method affects acoustic diversity for consistency models, in comparison with temperature sampling on its discrete counterpart. More precisely, we compute WavLM speaker embeddings (Chen et al., 2021) over 100 unprompted speech generations with different values of temperature, both for an RQ-transformer and CALM. In both cases, the inner monologue text stream is generated with 0.8 temperature to ensure text diversity. We then average the pairwise cosine similarities of these embeddings, as a measure of diversity: the higher the average similarity, the lower speaker diversity in generated audio. The reference speaker similarity number is computed over 100 examples from the ground truth dataset. Fig. 3 shows, as expected, that speaker similarity tends to decrease with temperature, which means that temperature increases diversity with a similar trajectory to the discrete models.
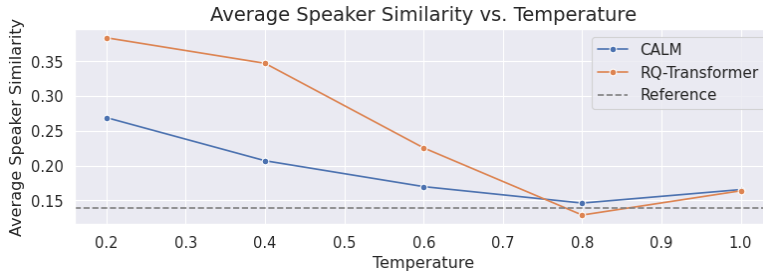

Figure 3: Average pairwise speaker similarity over 100 unprompted 10s generations, or 100 10s examples from the ground truth dataset as reference. As expected, for both methods models generate more diverse speakers (i.e. less pairwise speaker similarity) as temperature increases.

6 Conclusion

We present *Continuous Audio Language Models* (CALM), a novel framework for autoregressive audio generation that operates directly in the continuous latent space of a VAE, bypassing the limitations of discrete quantization. Replacing RVQ or diffusion heads with consistency models significantly reduces inference cost while improving sample quality as shown by our experiments. Our architecture combines noise-injected long-term context and clean short-term context, implemented via a dual-transformer design. We introduce practical innovations such as temperature sampling and a head batch multiplier to further improve sampling quality and training efficiency. We demonstrate the effectiveness of our approach across both speech and music generation tasks. Our results suggest that continuous modeling offers a compelling alternative to discrete tokenization for high-quality, efficient, and scalable autoregressive audio generation.

References

Andrea Agostinelli, Timo I. Denk, Zalán Borsos, Jesse Engel, Mauro Verzetti, Antoine Caillon, Qingqing Huang, Aren Jansen, Adam Roberts, Marco Tagliasacchi, Matt Sharifi, Neil Zeghidour, and Christian Frank. Musiclm: Generating music from text, 2023. URL `https://arxiv.org/abs/2301.11325`.

Zalán Borsos, Raphaël Marinier, Damien Vincent, Eugene Kharitonov, Olivier Pietquin, Matt Sharifi, Dominik Roblek, Olivier Teboul, David Grangier, Marco Tagliasacchi, and Neil Zeghidour. Audiolm: a language modeling approach to audio generation, 2023. URL `https://arxiv.org/abs/2209.03143`.

Ralph Allan Bradley and Milton E. Terry. Rank analysis of incomplete block designs: The method of paired comparisons. *Biometrika*, 39(3-4):324–345, 12 1952. ISSN 0006-3444. doi: 10.1093/biomet/39.3-4.324. URL `https://doi.org/10.1093/biomet/39.3-4.324`.

Francois Caron and Arnaud Doucet. Efficient bayesian inference for generalized bradley-terry models, 2010. URL `https://arxiv.org/abs/1011.1761`.

Sanyuan Chen, Chengyi Wang, Zhengyang Chen, Yu Wu, Shujie Liu, Zhuo Chen, Jinyu Li, Naoyuki Kanda, Takuya Yoshioka, Xiong Xiao, Jian Wu, Long Zhou, Shuo Ren, Yanmin Qian, Yao Qian, Jian Wu, Michael Zeng, and Furu Wei. Wavlm: Large-scale self-supervised pre-training for full stack speech processing. *CoRR*, abs/2110.13900, 2021. URL `https://arxiv.org/abs/2110.13900`.

Michael Chinen, Felicia S. C. Lim, Jan Skoglund, Nikita Gureev, Feargus O'Gorman, and Andrew Hines. Visqol v3: An open source production ready objective speech and audio metric, 2020. URL `https://arxiv.org/abs/2004.09584`.

Jade Copet, Felix Kreuk, Itai Gat, Tal Remez, David Kant, Gabriel Synnaeve, Yossi Adi, and Alexandre Défossez. Simple and controllable music generation. In *Neurips*, 2023.

Prafulla Dhariwal, Heewoo Jun, Christine Payne, Jong Wook Kim, Alec Radford, and Ilya Sutskever. Jukebox: A generative model for music, 2020. URL `https://arxiv.org/abs/2005.00341`.

Alexandre Défossez, Jade Copet, Gabriel Synnaeve, and Yossi Adi. High fidelity neural audio compression. In *ICLR*, 2024a.

Alexandre Défossez, Laurent Mazaré, Manu Orsini, Amélie Royer, Patrick Pérez, Hervé Jégou, Edouard Grave, and Neil Zeghidour. Moshi: a speech-text foundation model for real-time dialogue, 2024b. URL `https://arxiv.org/abs/2410.00037`.

Zach Evans, CJ Carr, Josiah Taylor, Scott H. Hawley, and Jordi Pons. Fast timing-conditioned latent audio diffusion. In *ISMIR*, 2024.

Lijie Fan, Tianhong Li, Siyang Qin, Yuanzhen Li, Chen Sun, Michael Rubinstein, Deqing Sun, Kaiming He, and Yonglong Tian. Fluid: Scaling autoregressive text-to-image generative models with continuous tokens. In *ICLR*, 2025.

Kevin Frans, Danijar Hafner, Sergey Levine, and Pieter Abbeel. One step diffusion via shortcut models. In *ICLR*, 2025.

Jiatao Gu, Yuyang Wang, Yizhe Zhang, Qihang Zhang, Dinghuai Zhang, Navdeep Jaitly, Josh Susskind, and Shuangfei Zhai. Dart: Denoising autoregressive transformer for scalable text-to-image generation, 2025.

Yiwei Guo, Zhihan Li, Hankun Wang, Bohan Li, Chongtian Shao, Hanglei Zhang, Chenpeng Du, Xie Chen, Shujie Liu, and Kai Yu. Recent advances in discrete speech tokens: A review, 2025. URL `https://arxiv.org/abs/2502.06490`.

Tiankai Hang, Jianmin Bao, Fangyun Wei, and Dong Chen. Fast autoregressive models for continuous latent generation, 2025. URL `https://arxiv.org/abs/2504.18391`.

Jonathan Ho, Ajay Jain, and Pieter Abbeel. Denoising diffusion probabilistic models. In *NeurIPS*, 2020.

Dongya Jia, Zhuo Chen, Jiawei Chen, Chenpeng Du, Jian Wu, Jian Cong, Xiaobin Zhuang, Chumin Li, Zhen Wei, Yuping Wang, and Yuxuan Wang. Ditar: Diffusion transformer autoregressive modeling for speech generation, 2025. URL `https://arxiv.org/abs/2502.03930`.

Albert Q. Jiang, Alexandre Sablayrolles, Arthur Mensch, Chris Bamford, Devendra Singh Chaplot, Diego de las Casas, Florian Bressand, Gianna Lengyel, Guillaume Lample, Lucile Saulnier, Lélio Renard Lavaud, Marie-Anne Lachaux, Pierre Stock, Teven Le Scao, Thibaut Lavril, Thomas Wang, Timothée Lacroix, and William El Sayed. Mistral 7b, 2023. URL `https://arxiv.org/abs/2310.06825`.

Eugene Kharitonov, Damien Vincent, Zalán Borsos, Raphaël Marinier, Sertan Girgin, Olivier Pietquin, Matt Sharifi, Marco Tagliasacchi, and Neil Zeghidour. Speak, read and prompt: High-fidelity text-to-speech with minimal supervision. *Transactions of the Association for Computational Linguistics*, 11:1703–1718, 2023.

Felix Kreuk, Gabriel Synnaeve, Adam Polyak, Uriel Singer, Alexandre Défossez, Jade Copet, Devi Parikh, Yaniv Taigman, and Yossi Adi. Audiogen: Textually guided audio generation, 2023. URL `https://arxiv.org/abs/2209.15352`.

Rithesh Kumar, Prem Seetharaman, Alejandro Luebs, Ishaan Kumar, and Kundan Kumar. High-fidelity audio compression with improved rvqgan. In *NeurIPS*, 2023.

Kyutai. Helium 1: a modular and multilingual llm. `https://kyutai.org/2025/04/30/helium.html`, april 2025. Blog post.

Tom Labiausse, Laurent Mazaré, Edouard Grave, Patrick Pérez, Alexandre Défossez, and Neil Zeghidour. High-fidelity simultaneous speech-to-speech translation. In *ICML*, 2025.

Kushal Lakhotia, Evgeny Kharitonov, Wei-Ning Hsu, Yossi Adi, Adam Polyak, Benjamin Bolte, Tu-Anh Nguyen, Jade Copet, Alexei Baevski, Adelrahman Mohamed, and Emmanuel Dupoux. Generative spoken language modeling from raw audio. In *TACL*, 2021.

Doyup Lee, Chiheon Kim, Saehoon Kim, Minsu Cho, and Wook-Shin Han. Autoregressive image generation using residual quantization, 2022. URL `https://arxiv.org/abs/2203.01941`.

Jean-Marie Lemercier, Simon Rouard, Jade Copet, Yossi Adi, and Alexandre Défossez. An independence-promoting loss for music generation with language models. In *ICML*, 2024.

Tianhong Li, Yonglong Tian, He Li, Mingyang Deng, and Kaiming He. Autoregressive image generation without vector quantization. In *Neurips*, 2024.

Yaron Lipman, Ricky T. Q. Chen, Heli Ben-Hamu, Maximilian Nickel, and Matt Le. Flow matching for generative modeling. In *ICLR*, 2023.

Chen-Chou Lo, Szu-Wei Fu, Wen-Chin Huang, Xin Wang, Junichi Yamagishi, Yu Tsao, and Hsin-Min Wang. Mosnet: Deep learning-based objective assessment for voice conversion. In *Interspeech 2019*, interspeech_2019. ISCA, September 2019. doi: 10.21437/interspeech.2019-2003. URL `http://dx.doi.org/10.21437/Interspeech.2019-2003`.

Cheng Lu and Yang Song. Simplifying, stabilizing and scaling continuous-time consistency models. In *ICLR*, 2025.

OpenAI. Gpt-4 technical report, 2024. URL `https://arxiv.org/abs/2303.08774`.

Myle Ott, Sergey Edunov, Alexei Baevski, Angela Fan, Sam Gross, Nathan Ng, David Grangier, and Michael Auli. fairseq: A fast, extensible toolkit for sequence modeling. In *Proceedings of NAACL-HLT 2019: Demonstrations*, 2019.

Marco Pasini, Stefan Lattner, and George Fazekas. Music2latent: Consistency autoencoders for latent audio compression. In *ISMIR*, 2024a.

Marco Pasini, Javier Nistal, Stefan Lattner, and George Fazekas. Continuous autoregressive models with noise augmentation avoid error accumulation. In *NeurIPS Audio Imagination Workshop*, 2024b.

Marco Pasini, Stefan Lattner, and György Fazekas. Music2latent2: Audio compression with summary embeddings and autoregressive decoding. In *ICASSP 2025 - 2025 IEEE International Conference on Acoustics, Speech and Signal Processing (ICASSP)*, pp. 1–5, 2025.

Alec Radford, Jong Wook Kim, Tao Xu, Greg Brockman, Christine McLeavey, and Ilya Sutskever. Robust speech recognition via large-scale weak supervision, 2022. URL `https://arxiv.org/abs/2212.04356`.

Thomas Schatz, Vijayaditya Peddinti, Francis Bach, Aren Jansen, Hynek Hermansky, and Emmanuel Dupoux. Evaluating speech features with the minimal-pair abx task: analysis of the classical mfc/plp pipeline. In *Interspeech 2013*, pp. 1781–1785, 2013. doi: 10.21437/Interspeech.2013-441.

Yang Song, Jascha Sohl-Dickstein, Diederik P. Kingma, Abhishek Kumar, Stefano Ermon, and Ben Poole. Score-based generative modeling through stochastic differential equations. In *ICLR*, 2021.

Yang Song, Prafulla Dhariwal, Mark Chen, and Ilya Sutskever. Consistency models. In *ICML*, 2023.

Hugo Touvron, Thibaut Lavril, Gautier Izacard, Xavier Martinet, Marie-Anne Lachaux, Timothée Lacroix, Baptiste Rozière, Naman Goyal, Eric Hambro, Faisal Azhar, Aurelien Rodriguez, Armand Joulin, Edouard Grave, and Guillaume Lample. Llama: Open and efficient foundation language models, 2023. URL `https://arxiv.org/abs/2302.13971`.

Michael Tschannen, Cian Eastwood, and Fabian Mentzer. Givt: Generative infinite-vocabulary transformers, 2024. URL `https://arxiv.org/abs/2312.02116`.

Arnon Turetzky, Nimrod Shabtay, Slava Shechtman, Hagai Aronowitz, David Haws, Ron Hoory, and Avihu Dekel. Continuous speech synthesis using per-token latent diffusion, 2024. URL `https://arxiv.org/abs/2410.16048`.

Aaron van den Oord, Sander Dieleman, Heiga Zen, Karen Simonyan, Oriol Vinyals, Alex Graves, Nal Kalchbrenner, Andrew Senior, and Koray Kavukcuoglu. Wavenet: A generative model for raw audio, 2016. URL `https://arxiv.org/abs/1609.03499`.

Aaron van den Oord, Oriol Vinyals, and Koray Kavukcuoglu. Neural discrete representation learning, 2018. URL `https://arxiv.org/abs/1711.00937`.

Ashish Vaswani, Noam Shazeer, Niki Parmar, Jakob Uszkoreit, Llion Jones, Aidan N. Gomez, and Lukasz Kaiser and. Attention is all you need. In *Advances in Neural Information Processing Systems (NeurIPS)*, pp. 5998–6008, 2017.

Chengyi Wang, Sanyuan Chen, Yu Wu, Ziqiang Zhang, Long Zhou, Shujie Liu, Zhuo Chen, Yanqing Liu, Huaming Wang, Jinyu Li, Lei He, Sheng Zhao, and Furu Wei. Neural codec language models are zero-shot text to speech synthesizers, 2023. URL `https://arxiv.org/abs/2301.02111`.

Dongchao Yang, Jinchuan Tian, Xu Tan, Rongjie Huang, Songxiang Liu, Xuankai Chang, Jiatong Shi, Sheng Zhao, Jiang Bian, Xixin Wu, et al. Uniaudio: An audio foundation model toward universal audio generation. *arXiv preprint arXiv:2310.00704*, 2023.

Neil Zeghidour, Alejandro Luebs, Ahmed Omran, Jan Skoglund, and Marco Tagliasacchi. Soundstream: An end-to-end neural audio codec. *CoRR*, abs/2107.03312, 2021. URL `https://arxiv.org/abs/2107.03312`.

A   Supplementary Experiments

A.1   Short-context transformer window

To study the influence of the context window K of the short-context transformer, we performed an hyperparameter search with $K = 5, 10, 20, 40$ and trained our models for 500K training steps. We observe that finding an optimal value of K is not critical even though it seems that 5 is not enough.

Table 7: **FAD after 500K training steps for different short-context Transformer contexts K.**

K in short-context Transformer	FAD
5	0.85 ± 0.05
10	0.76 ± 0.04
20	0.73 ± 0.04
40	0.78 ± 0.04

A.2   Scalability of CALM

In order to see if all the hyperparameters of our CALM method transfer well to more model parameters, we trained a consistency music CALM model with a larger 3B backbone (with a model dimension of 2048, 32 heads and 48 layers) as well as a discrete RQ-Transformer with 32-RVQ model with the same backbone size. For the CALM model, we use 4 consistency steps at inference. The results are as follow (we compare with the main model that has a 1.3B backbone):

Table 8: **Scalability of the backbone for CALM and RQ-Transformer methods.**

Model	FAD
CALM with 3B backbone	0.62 ± 0.05
32 RVQ RQ-Transformer with 3B backbone	0.98 ± 0.06
CALM with 1.3B backbone	0.71 ± 0.05
32 RVQ RQ-Transformer with 1.3B backbone	1.06 ± 0.06

B   Human evaluation methods

Audio clips are always 30s second total, with a 3s prompt coming from a ground truth audio. Each experiments has 50 samples for each method. There are 50 raters. Each of them sees 10 samples. Raters were payed £9 / hour for their contribution.

B.1   Speech continuation

Acoustic quality assessment: How would you rate the overall quality of this audio clip? Consider aspects such as clarity, balance, richness, and naturalness. Listen to at least 10 seconds of audio before deciding. 1 clip is presented, possibilities are bad, poor, fair, good, excellent.

Meaningfulness: Which of these two audio clips feels more like meaningful and natural speech? The first 3 seconds are identical. Listen to at least 10 seconds of each clip. 2 clips are presented, ties are possible. Elo scores are Bayesian estimates of the posterior mean in a Bradley-Terry model.

B.2   Music continuation

Acoustic quality assessment: How would you rate the overall quality of this music? Consider aspects such as clarity, balance, richness, and naturalness. Listen to at least 10 seconds of audio before deciding. 1 clip is presented, possibilities are bad, poor, fair, good, excellent.

Music enjoyment: Which music do you enjoy listening to more? The first 3 seconds are identical. Listen to at least 10 seconds of each clip. 2 clips are presented, ties are possible. Elo scores are Bayesian estimates of the posterior mean in a Bradley-Terry model.

B.3 Bayesian Elo Score

The Meaningfulness metric for speech and the Enjoyment metric for music are both Bayesian Elo Scores. Elo score is used to rank models based on some pairwise comparisons of audio samples. Given two models A and B, the probability that A is preferred over B is:

$$P(A > B) = \frac{1}{1 + 10^{(E_B - E_A)/400}} \qquad (4)$$

where E_A and E_B are the Elo scores of each model. Unlike a traditional Elo score, the Bayesian Elo score uses a Gamma prior, so that one can derive confidence intervals over the posterior distribution. By defining S_A such as $E_A = 400 \log_{10}(S_A) + c$ with c being a constant, we obtain:

$$P(A > B) = \frac{S_A}{S_A + S_B} \qquad (5)$$

which is a Bradley-Terry (Bradley & Terry, 1952) model. There are a few different methods to estimate the parameters of a Bradley-Terry model. We use the iterative one from (Caron & Doucet, 2010) where S_A^0 follows a Gamma prior with parameters α^0, β^0. By denoting w_A the number of times where method A won against any other methods and n_{AB} the number of times where A and B are compared, S_A^t is computed with the following update rule until convergence:

$$S_A^{t+1} = \frac{\alpha + w_A}{\beta + \sum_{B \neq A} \frac{n_{AB}}{S_A^t + S_B^t}} \qquad (6)$$

which is the mean of the Gamma distribution with updated parameters $\alpha_A^{t+1}, \beta_A^{t+1}$:

$$\alpha_A^{t+1} = \alpha^0 + w_A, \qquad \text{and} \qquad \beta_A^{t+1} = \beta^0 + \sum_{B \neq A} \frac{w_{A,B}}{S_A^t + S_B^t}. \qquad (7)$$

Iterating over t allows to reach a fix point, we run 30 of them, once we have collected all the pairs. We use $\alpha = 0.1, \beta = 0.1, c = 2000$ so that in absence of any data, $S_A = 1$ and $E_A = 2000$. Confidence interval are 95% confidence interval according to the posterior (the 2.5th and 97.5th percentiles).

C Hyperparameters

We present in Tab. 10 the parameters of the music and speech VAE used for CALMs. For CALMs and the RQ-Transformer based discrete LMs, the hyperparameters are presented in Tab. 9.

Table 9: Model and training hyperparameters

	Music continuation	Speech continuation
Backbone Transformer		
Model dimension	1536	2560
MLP dimension	6336	10560
Number of heads	24	20
Number of layers	48	24
Learning rate	$1 \cdot 10^{-4}$	$5 \cdot 10^{-5}$
Number of parameters	1.35B	2.2B
RQ-Transformer head (RVQ model)		
Model dimension	1024	1024
MLP dimension	4096	4096
Number of heads	16	16
Number of layers	6	6
Number of parameters	701M	701M
Consistency sampler head (ours)		
Number of layers	12	6
MLP dimension	3072	512
Gating	SiLU	SiLU
Number of parameters	601M	10M
Short context transformer (ours)		
Model dimension	1536	✗
MLP dimension	6336	✗
Number of heads	24	✗
Number of layers	4	✗
Context	10	✗
Number of parameters	113M	✗
Audio embedding manipulations		
Center and normalize	✓	✓
Noise before entering backbone	✓	✗
Training parameters		
Head batch multiplier	8	8
Optimizer	AdamW $\beta_1 = 0.9, \beta_2 = 0.95$	AdamW $\beta_1 = 0.9, \beta_2 = 0.95$
Batch size	48	144
Audio sample length	30s	300s
LR Schedule	cosine	cosine
Learning rate	$1 \cdot 10^{-4}$	$2 \cdot 10^{-4}$
GPU used	16 H100	48 H100
Number of training steps	500k	150k
Initial checkpoint	✗	Helium-1 (Kyutai, 2025)
Inner monologue	✗	✓
Acoustic delay	-	2 frames (160 ms)

Table 10: VAE hyperparameters

	Music VAE	Speech VAE
General		
Sample rate	32kHz	24kHz
Frame rate	25Hz	12.5Hz
Latent dimension	128	32
Architecture		
Convolutions ratios	8, 8, 5, 4	6, 5, 4, 4, 4
Num transformer encoder layers	4	8
Num transformer decoder layers	4	8
Transformer context	30s	10s
Training parameters		
Batch size	64	64
Audio sample length	12s	12s
KL loss weight	0.01	0.01
Reconstruction loss	✓	✗
Distillation loss weight	✗	25
LR Schedule	cosine	cosine
Learning rate	$8 \cdot 10^{-4}$	$8 \cdot 10^{-4}$